

A Levelized Comparison of Pulsed and Steady-State Tokamaks

by

Daniel Joseph Segal

B.S. Engineering Physics, University of Wisconsin (2014)

Submitted to the Department of Nuclear Science and Engineering
in partial fulfillment of the requirements for the degree of

Master of Science in Nuclear Science and Engineering

at the

MASSACHUSETTS INSTITUTE OF TECHNOLOGY

February 2019

© Massachusetts Institute of Technology 2019. All rights reserved.

Author

Department of Nuclear Science and Engineering
January 5, 2019

Certified by

Jeffrey P. Freidberg
KEPCO Professor Emeritus
Thesis Supervisor

Certified by

Anne E. White
Cecil and Ida Green Associate Professor
Thesis Reader

Accepted by

Ju Li
Battelle Energy Alliance Professor
Chair, Department Committee on Graduate Students

A Levelized Comparison of Pulsed and Steady-State Tokamaks

by

Daniel Joseph Segal

Submitted to the Department of Nuclear Science and Engineering
on January 5, 2019, in partial fulfillment of the
requirements for the degree of
Master of Science in Nuclear Science and Engineering

Abstract

The goal of fusion energy research is to build an economically competitive reactor. This is difficult due to the complicated system composing a reactor and the nonlinearities it entails. Practically, to even get to the neighborhood of an economic reactor requires hundreds of simulations – which in turn necessitate quick running fusion systems codes. Moving towards these economic reactors then involves finding what design parameters provide the most leverage in lowering reactor costs.

As highlighted by the difference between European and American designs, however, the most important decision for tokamaks is whether to run them as *pulsed* or *steady-state*. This paper aims to fairly compare the two modes of operation using a single, comprehensive model. Benchmarked against other codes, this model actually shows that no fusion reactor is achievable without some technological advancements. This can be seen through every referenced design using nonstandard values of H and N_G .

The interesting result this paper shows is that developing high-temperature superconducting (HTS) tape could actually make both steady-state and pulsed tokamaks economically competitive against solar and coal. Further, this HTS tape actually has different best uses for the two modes of operation, appearing in the magnet structures of: TF coils for steady state and the central solenoid for pulsed. Developments in this technology should produce economic reactors within the coming decade.

Thesis Supervisor: Jeffrey P. Freidberg

Title: Professor of Nuclear Science and Engineering (Emeritus)

Contents

1	Introducing Fusion Reactor Design	17
1.1	Distinguishing Pulsed from Steady-State	18
1.2	Pricing a Fusion Reactor	19
1.3	Modeling Fusion Systems	21
1.4	Discussing HTS Magnet Technology	22
2	Designing a Steady-State Tokamak	25
2.1	Defining Plasma Parameters	26
2.1.1	Understanding Tokamak Geometry	26
2.1.2	Prescribing Plasma Profiles	28
2.2	Solving the Steady Current	31
2.2.1	Enforcing the Greenwald Density Limit	31
2.2.2	Declaring the Bootstrap Current	34
2.2.3	Deriving the Fusion Power	35
2.2.4	Using Current Drive	37
2.2.5	Completing the Steady Current	38
2.3	Handling Current Drive Self-Consistently	39
3	Formalizing the Systems Model	41
3.1	Explaining Static Variables	42
3.2	Connecting Dynamic Variables	42
3.3	Enforcing Power Balance	46
3.3.1	Collecting Power Sources	46
3.3.2	Approximating Radiation Losses	48

3.3.3	Estimating Heat Conduction Losses	49
3.3.4	Writing the Lawson Parameter	51
3.3.5	Finalizing the Primary Constraint	53
3.4	Collecting Limiting Constraints	56
3.4.1	Introducing the Beta Limit	56
3.4.2	Giving the Kink Safety Factor	58
3.4.3	Working under the Wall Loading Limit	58
3.4.4	Setting a Maximum Power Cap	60
3.4.5	Listing the Heat Loading Limit	61
3.5	Summarizing the Fusion Systems Model	62
4	Designing a Pulsed Tokamak	65
4.1	Modeling Plasmas as Circuits	66
4.1.1	Drawing the Circuit Diagram	66
4.1.2	Plotting Pulse Profiles	68
4.1.3	Specifying Circuit Variables	72
4.1.4	Constructing the Pulse Length	76
4.2	Producing Flux Balance	77
4.2.1	Rearranging the Circuit Equation	78
4.2.2	Adding Poloidal Field Coils	79
4.3	Improving Tokamak Geometry	81
4.3.1	Defining Central Solenoid Dimensions	81
4.3.2	Calculating Component Thicknesses	82
4.3.3	Revisiting Central Solenoid Dimensions	85
4.4	Piecing Together the Generalized Current	87
4.5	Simplifying the Generalized Current	88
4.5.1	Recovering the Steady Current	88
4.5.2	Extracting the Pulsed Current	89
4.5.3	Rationalizing the Generalized Current	90

5	Completing the Systems Model	93
5.1	Describing a Simple Algebra	93
5.2	Generalizing Previous Equations	95
5.2.1	Including Limiting Constraints	95
5.2.2	Minimizing Intermediate Quantities	97
5.2.3	Pinning Dynamic Variables	98
5.2.4	Detailing the Equation Solver	98
5.3	Wrapping up the Logic	101
6	Presenting the Code Results	103
6.1	Testing the Code against other Models	104
6.1.1	Comparing with the PSFC ARC Reactor	105
6.1.2	Contrasting with the ARIES ACT Studies	106
6.1.3	Benchmarking with the Process DEMO Designs	108
6.2	Developing Prototype Reactors	115
6.2.1	Navigating around Charybdis	119
6.2.2	Pinning down Proteus	119
6.2.3	Highlighting Operation Differences	120
6.3	Learning from the Data	120
6.3.1	Picking a Design Point	120
6.3.2	Utilizing High Field Magnets	125
6.3.3	Looking at Design Alternatives	128
7	Planning Future Work for the Model	135
7.1	Incorporating Stellarator Technology – Ladon	135
7.2	Making a Composite Reactor – Janus	136
7.3	Bridging Confinement Scalings – Daedalus	137
7.4	Addressing Model Shortcomings	138
7.4.1	Integrating Pedestal Temperature Profiles	139
7.4.2	Expanding the Radiation Loss Term	139
7.4.3	Taking Flux Sources Seriously	139

8	Concluding Reactor Discussion	141
A	Cataloging Model Variables	143
A.1	Static Variables	143
A.2	Dynamic Variables	144
A.3	Intermediate Variables	144
B	Simulating with Fussy.jl	145
B.1	Getting the Code to Work	145
B.2	Sorting out the Codebase	146
B.2.1	Typing out Structures	147
B.2.2	Referencing Input Decks and Solutions	149
B.2.3	Acknowledging Utility Functions	149
B.2.4	Mentioning Base Level Files	149
B.3	Delving into Reactor Methods	150
B.4	Demonstrating Code Usage	151
B.4.1	Initializing the Workspace	152
B.4.2	Running a Study	152
B.4.3	Extracting Results	153
B.4.4	Plotting Curves	154
C	Discussing Fusion Power	159
C.1	Theoretical Background	159
C.2	Bosch-Hale Reactivity	161
D	Selecting Plasma Profiles	165
D.1	Density – n	165
D.2	Temperature – T	167
D.3	Pressure – p	169
D.4	Bootstrap Current – f_{BS}	169
D.5	Volume Averaged Powers	171

E	Determining Plasma Flux Surfaces	173
E.1	Flux Surface Coordinates	174
E.2	Cross-sectional Area and Volume	175
E.3	Surface and Volume Integrals	176
F	Expanding on the Bootstrap Current	179
F.1	Summarized Results	179
F.2	Detailed Analysis	181
G	Elaborating on the Current Drive	187
G.1	Summarized Results	187
G.2	Detailed Analysis	188
H	Compending Code Plots	197
H.1	Magnet Strength Scans	198
H.2	Cost Sensitivity Studies	219
	References	235

List of Figures

1-1	Cut-Away of Tokamak Reactor	18
1-2	Comparison of Pulsed and Steady-State Current	19
1-3	Steady State Magnet Components	23
1-4	Pulsed Magnet Components	23
2-1	Geometry of a Tokamak	27
2-2	Geometric Parameters	28
2-3	Radial Plasma Profiles	29
2-4	Greenwald Density Limit	33
3-1	Current Balance in a Tokamak	45
3-2	Power Balance in a Reactor	52
3-3	H-Mode Confinement Time Scaling	54
4-1	A Simple Plasma Transformer Description	67
4-2	Time Evolution of Circuit Profiles	69
4-3	Dimensions of Tokamak Cross-Section	82
5-1	Equation Selection for Fusion System	94
5-2	Minimize Cost Step II/III – Optimize Reactor	99
6-1	ARC and ACT Studies Cost Dependence on the H Factor	107
6-2	ARC Model Comparison	110
6-3	ARIES ACT I Model Comparison	111
6-4	ARIES ACT II Model Comparison	112
6-5	DEMO Steady Model Comparison	113

6-6	DEMO Pulsed Model Comparison	114
6-7	Designing Reactor Prototypes	116
6-8	Steady State Prototype Comparison	117
6-9	Pulsed Prototype Comparison	118
6-10	Limiting Constraint Regimes	121
6-11	Steady State Cost Curves	123
6-12	Pulsed Cost Curves	124
6-13	Pulsed B_{CS} Sensitivities	126
6-14	Pulsed Monte Carlo Sampling	127
6-15	Bootstrap Current Monte Carlo Sampling	129
6-16	Internal Inductance Sensitivities	130
6-17	Pulsed H Sensitivities	132
6-18	Steady State Current Drive Efficiency	133
6-19	Current Drive Efficiency vs Launch Angle	134
7-1	Cut-Away of Stellarator Reactor	136
7-2	Current Balance in a Tokamak	137
B-1	A Blank Plot	155
B-2	An Empty Plot	156
B-3	An Unscaled Plot	156
B-4	A Scaled Plot	157
C-1	Comparing Nuclear Fusion and Fission	160
C-2	The D-T Fusion Reaction	161
D-1	Radial Plasma Profiles	165
E-1	Cut-Away of Tokamak Reactor	173
E-2	Dimensions of Tokamak Cross-Section	176

List of Tables

3.1	Dynamic Variables	42
4.1	Piecewise Linear Scheme for Pulsed Operation	69
4.2	Example TF Coils and Central Solenoid Critical Values	84
5.1	Main Equation Bank	96
6.1	ARC Variables	110
6.2	ACT I Variables	111
6.3	ACT II Variables	112
6.4	DEMO Steady Variables	113
6.5	DEMO Pulsed Variables	114
6.6	Charybdis Variables	117
6.7	Proteus Variables	118
6.8	Proteus and Charybdis Comparison	119
A.1	List of Static Variables	143
A.2	List of Dynamic Variables	144
A.3	List of Intermediate Variables (Noncomprehensive)	144
C.1	Bosch-Hale Parametrization Coefficients	163
C.2	Tabulated Bosch-Hale Reactivities	163

List of Equations

1.1	Magnetic Energy – W_M	20
1.3	Cost-per-Watt – C_W	21
2.1	Minor Radius – a	27
2.2	Density Profile – n	29
2.4	Temperature Profile – T	30
2.5	Current Density Profile – J	30
2.6	Normalized Poloidal Magnetic Field – b_p	31
2.7	Current Balance – I	31
2.10	Greenwald Density – \bar{n}	32
2.14	Bootstrap Current – I_{BS}	35
2.19	Dilution Factor – f_D	36
2.21	Fusion Power – P_F	36
2.25	Heating Power – P_H	38
2.26	Current Drive – I_{CD}	38
2.28	Steady Current – I_P	39
2.29	Current Drive Efficiency – η_{CD}	40
3.1	Scanned Temperature – \bar{T}	43
3.3	Current Fractions – f	44
3.6	Power Balance – P	46
3.8	Plasma Resistance – R_P	47
3.10	Ohmic Power – P_Ω	47
3.15	Bremsstrahlung Power – P_{BR}	49
3.20	Heat Conduction Losses – P_κ	50
3.23	Triple Product – $\bar{n} \cdot \bar{T} \cdot \tau_E$	52

3.25	Generalized Confinement Time Scaling Law – τ_E	53
3.26	Loss Power – P_{src}	54
3.27	ELMy H-Mode Confinement Time Scaling Law – τ_E^H	55
3.28	Primary Constraint – B_0	55
3.35	Plasma Pressure – \bar{p}	57
3.38	Troyon Beta Limit – β_N	57
3.41	Kink Safety Factor – q_*	58
3.43	Surface Area – S_P	59
3.45	Wall Loading Limit – P_W	59
3.47	Electric Power – P_E	60
3.51	Maximum Power Limit – P_{max}	61
3.55	Heat Loading Limit – q_{DV}	62
4.12	Ramp-Up Time – τ_{RU}	70
4.16	Flat-top Time – τ_{FT}	71
4.17	Ramp-Down Time – τ_{RD}	71
4.19	Dwell Time – τ_{DW}	72
4.20	Duty Factor – f_{duty}	73
4.23	Inductive Current – I_{ID}	74
4.26	Central Solenoid Inductance – L_1	75
4.29	Plasma Inductance – L_2	75
4.34	Mutual Inductance – M	76
4.40	Central Solenoid Flux – Φ_{CS}	78
4.42	Ramp-Up Flux – Φ_{RU}	79
4.43	Flat-top Flux – Φ_{FT}	79
4.44	PF Coil Flux – Φ_{PF}	79
4.48	Plasma Perimeter – l_p	80
4.50	Vertical Field Strength – B_V	80
4.53	Flux Balance – Φ	81
4.56	Blanket Thickness – b	83
4.57	TF Coil Thickness – c	83

4.61	Central Solenoid Thickness – d	84
4.64	Central Solenoid Height – h_{CS}	85
4.65	Central Solenoid Inner Radius – R_{CS}	85
4.75	Generalized Current – I_P	88
5.3	General Model Equation – $G(\overline{T})$	95
5.10	General Model Solution – $\gamma_{RB\{I,T\}}$	100
7.1	L-Mode Confinement Time Scaling Law – τ_E^L	138
7.2	I-Mode Confinement Time Scaling Law – τ_E^I	138
C.2	Fusion Energy – E_F	160
C.3	Neutron Power – P_n	160
C.4	Alpha Power – P_α	160
C.9	Bosch-Hale Reactivity – $\langle\sigma v\rangle$	162
E.14	Shaping Parameter – g	175
E.24	Volume Integral – Q_V	177
E.25	Surface Integral – Q_S	177
F.7	Internal Inductance – l_i	180

Chapter 4

Designing a Pulsed Tokamak

Pulsed tokamaks are the flagship of the European fusion reactor-design effort. As such, this paper's model will now be generalized to accommodate this mode of operation. Fundamentally, this involves transforming current balance into flux balance – by adding inductive (pulsed) sources to stand alongside the LHCD (steady-state) ones.

The first step in generalizing current balance will be understanding the problem from a basic electrical engineering perspective – i.e. with circuit analysis. The resulting equation will then be transformed into the flux balance seen in other models from the literature.⁷ All that will need to be done then is solving the problem for plasma current (I_P) and simplifying it for various situations – e.g. steady-state operation.

This generalized plasma current will then be found to be a function of the other dynamic variables (i.e. R_0 , B_0 , and \bar{T}). This, of course, is more difficult to handle computationally than the steady current, which only depended directly on the temperature (\bar{T}). A discussion about solving this new root solving problem will be the topic of the next chapter.

4.1 Modeling Plasmas as Circuits

Although it may have been lost along the way, what makes plasmas so interesting and versatile – in comparison to gases – is their ability to respond to electric and magnetic fields. It seems natural then to model plasma current from a circuits perspective (i.e. with resistors, voltage sources, and inductors). By name, this circuit is referred to as a transformer where: the plasma is the secondary and the yet-to-be discussed central solenoid (of the tokamak) is the primary.

The first step in deriving a current equation is to determine the circuit equations that govern pulsed operation in a tokamak. This will be done in two steps. First, we will draw a circuit diagram and write equations that describe it. Next, we will use a simple schematic for how current evolves in a transformer to reduce the resulting differential equations to simple algebraic ones – as is the hallmark of our model.

4.1.1 Drawing the Circuit Diagram

Understanding a circuit always starts with drawing a simple diagram, see Fig. 4-1. This figure depicts the transformer governing a pulsed reactor. The left sub-circuit is, therefore, the transformer's primary: the central solenoid which provides most of the inductive current. Whereas, the right sub-circuit is the plasma acting as the transformer's secondary.*

This is handled with standard circuit equations for voltages, resistors, and inductors:¹¹

$$V_i = \sum_j^n \frac{d}{dt} (M_{ij} I_j) + I_i R_i , \quad \forall i = 1, 2, \dots, n \quad (4.1)$$

Without going into the inductances (M) and resistances (R), the variable n is the number of sub-circuits, here being 2. Whereas, the variables i and j are the indices of sub-circuits (i.e. 1 for the primary, 2 for the secondary). For illustrative purposes,

*The central solenoid is a coiled metal structure that fits within the inner ring of the tokamak enclosure. For now, every other flux source (besides this central solenoid) is neglected.

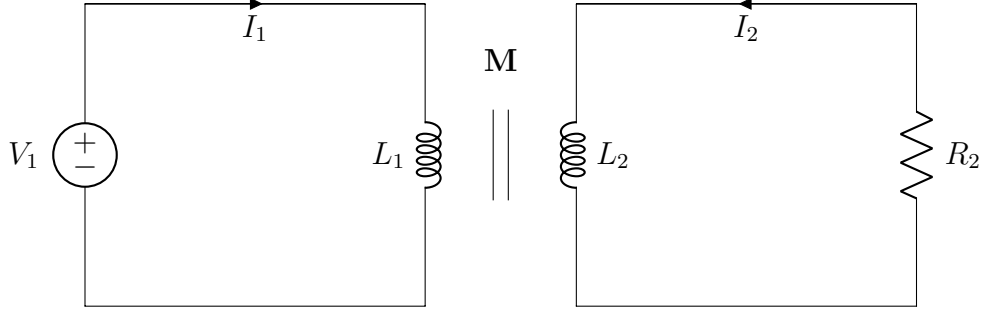


Figure 4-1: A Simple Plasma Transformer Description

A plasma transformer consists of a solenoid primary (left) and a plasma secondary (right). They are connected by their mutual inductance, M . Note, here, that the two currents – I_1 and I_2 – travel in opposite directions.

this would reduce to the following relation for a battery attached to a lightbulb:

$$V = IR \quad (4.2)$$

Back to the transformer diagram, the equations for the two subcircuits can be expanded and greatly simplified. Besides ignoring every inductive source other than the central solenoid, the next powerful assumption is treating the solenoid as a superconductor (i.e. with negligible resistance). Lastly, the inductances between components and themselves are held constant – independent of time. This allows the coupled transformer equations to be written as:

$$V_1 = L_1 \dot{I}_1 - M \dot{I}_2 \quad (4.3)$$

$$-I_2 R_P = L_2 \dot{I}_2 - M \dot{I}_1 \quad (4.4)$$

With I_1 and I_2 going in opposite directions. Note, here, that the subscript on M has been dropped, as there are only two components. This was done in conjunction to adding internal (self-)inductance terms. Mathematically, the mapping between variables is:

$$M = M_{12} = M_{21} \quad (4.5)$$

$$L_1 = M_{11} \tag{4.6}$$

$$L_2 = M_{22} \tag{4.7}$$

Repeated, the one subscript represents the primary – the central solenoid – and the two stands for the plasma as the transformer’s secondary. Exact definitions for the inductances will be put off until the end of the next subsection.

4.1.2 Plotting Pulse Profiles

Up until now, little has been discussed that has a time dependence. For steady-state tokamaks, this did not occur because it is an extreme case where pulses could last weeks or months. By definition, though, a pulsed machine has pulses – with around ten scheduled per day.³² For this reason, a fusion pulse is now investigated in detail.

Transformer pulses between the central solenoid and the plasma occur on the timescale of hours. During this time, a plasma is brought up to some quasi-steady-state current (I_P^*) for several hour and then ramped back down using the available flux in the solenoid (measured in volt-seconds). For clarity, each pulse is subdivided into four phases: ramp-up, flat-top, ramp-down, and dwell. Pictorially represented in Fig. 4-2, these divisions allow a simple scheme for transforming the coupled circuit differential equations – from Eqs. (4.3) and (4.4) – into simple algebraic formulas.

Along the way, we will approximate derivatives with linear piecewise functions. Using t_i to represent the initial time and t_f as the final one, these can be written as:

$$\dot{I} = \frac{I(t_f) - I(t_i)}{t_f - t_i} \tag{4.8}$$

Table 4.1 shows how this data from Fig. 4-2 can be written in this piecewise fashion.

The exact definitions for the plasma’s inductive current (I_P^*) and the maximum voltage in the central solenoid (V_{max}) will be put off until the end of the section.

Tokamak Circuit Profiles

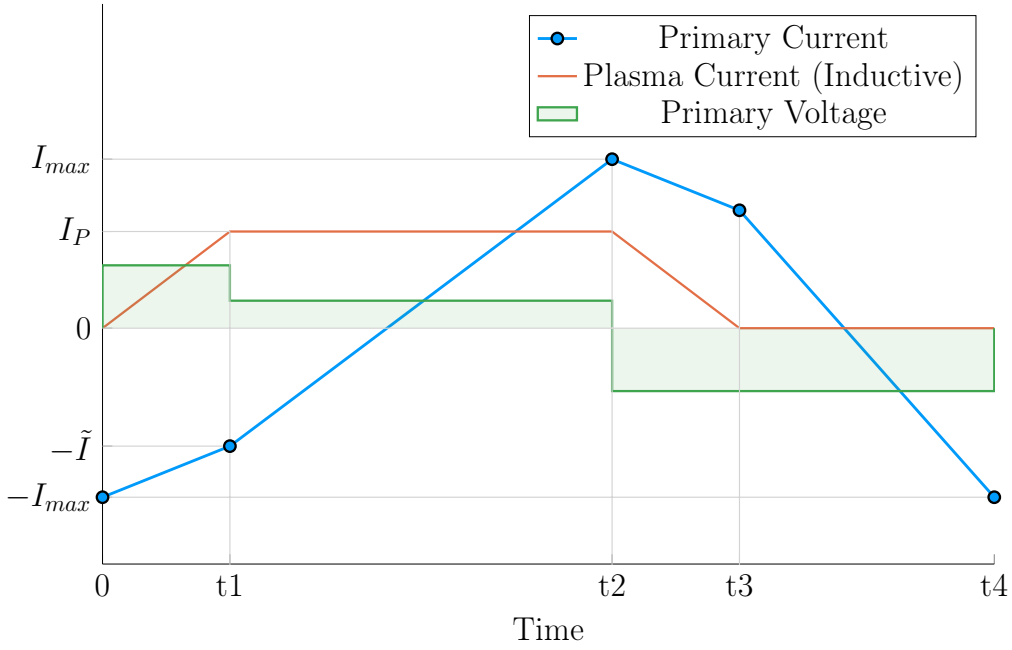


Figure 4-2: Time Evolution of Circuit Profiles

A circuit pulse involves four phases: (1) Ramp-Up, (2) Flattop, (3) Ramp-Down, and (4) Dwell. In reality, flattop can last more than 90% of the pulse.⁸ This makes the slope of the primary current during this phase much shallower than depicted.

The Ramp-Up Phase – RU

The first phase in every plasma pulse is the ramp-up. During ramp-up, the central solenoid starts discharging from its fully charged values, as the plasma is brought to its quasi-steady-state current. As this occurs on the timescale of minutes – not hours

Table 4.1: Piecewise Linear Scheme for Pulsed Operation

(a) Currents			(b) Voltage			
Time	I_1	I_2	Phase	t_i	t_f	V_1
0	$-I_{max}$	0	Ramp-Up	0	t_1	$+V_{max}$
t1	$-\tilde{I}$	I_P^*	Flattop	t_1	t_2	$+\tilde{V}$
t2	$+I_{max}$	I_P^*	Ramp-Down	t_2	t_3	$-V_{max}$
t3	$+\tilde{I}$	0	Dwell	t_3	t_4	$-V_{max}$
t4	$-I_{max}$	0				

– resistive effects of the plasma can safely be ignored. This results in the ramp-up equations becoming:

$$V_{max} = \frac{1}{\tau_{RU}} \cdot \left(L_1 \cdot (I_{max} - \tilde{I}) - M \cdot I_{ID} \right) \quad (4.9)$$

$$0 = \frac{1}{\tau_{RU}} \cdot \left(M \cdot (I_{max} - \tilde{I}) - L_2 \cdot I_{ID} \right) \quad (4.10)$$

Simplifying these equations will be done shortly, for now the new terms are what is important. The maximum voltage of the solenoid is V_{max} – usually measured in kilovolts. Next, I_{max} is the solenoid’s current at the beginning of ramp-up. Whereas \tilde{I} is the magnitude of the current once the plasma is at its flattop inductive-drive current – I_{ID} . The τ_{RU} quantity, then, is the duration of time it takes to ramp-up (i.e. RU). Again, L_1 and L_2 are the microhenry-scale internal inductances of the solenoid and plasma, respectively, and M is the mutual inductance between them.

The last step in discussing ramp-up is giving the two important formulas that come from it:

$$\tilde{I} = I_{max} - I_{ID} \cdot \left(\frac{L_2}{M} \right) \quad (4.11)$$

$$\tau_{RU} = \frac{I_{ID}}{V_{max}} \cdot \left(\frac{L_1 L_2 - M^2}{M} \right) \quad (4.12)$$

The Flattop Phase – FT

The most important phase in any reactor’s pulse is flattop: the quasi-steady-state time when the tokamak is making electricity. Flattops are assumed to last a few hours for a profitable machine, during which the central solenoid completely discharges to overcome a plasma’s resistive losses – thus, keeping it in a quasi-steady-state mode of operation. For a steady-state reactor, this phases constitutes the entirety of the pulse.

Although the resistance cannot be safely neglected for the flattop – as it was for ramp-up – the plasma’s inductive current (I_{ID}) is assumed constant. This leads to its derivative in equations cancelling out! Mathematically,

$$\tilde{V} = \frac{L_1}{\tau_{FT}} \cdot (I_{max} + \tilde{I}) \quad (4.13)$$

$$I_{ID}R_P = \frac{M}{\tau_{FT}} \cdot (I_{max} + \tilde{I}) \quad (4.14)$$

As with ramp-up, the simplifications will be given shortly. The new terms here, however, are an intermediate voltage for the central solenoid (\tilde{V}), and the duration of the flattop (τ_{FT}). The resistance term was given in Eq. (3.8). Solutions can now be found by substituting \tilde{I} – from Eq. (4.11) – into the flattop equations:

$$\tilde{V} = I_{ID}R_P \cdot \left(\frac{L_1}{M} \right) \quad (4.15)$$

$$\tau_{FT} = \frac{I_{max} \cdot 2M - I_{ID} \cdot L_2}{I_{ID}R_P} \quad (4.16)$$

The Ramp-Down Phase – RD

Due to the simplicity – and symmetry – of this model’s reactor pulse, ramp-down is the exact mirror of ramp-up. It takes the same amount of time and results in the same algebraic equations. For brevity, this will just be represented as:

$$\tau_{RD} = \tau_{RU} \quad (4.17)$$

For clarity, this is the time when a plasma’s current is brought down from its flattop value to zero.

The Dwell Phase – DW

Where the first three phases had little ambiguity, the dwell phase changes definition from model to model. For now, it is assumed to be the time it takes the central solenoid to reset after a plasma has been completely ramped-down to an off setting. To get a more realistic duty factor for cost estimates, it could include an evacuation time, set to last up to thirty minutes.¹² During this evacuation, a plasma is vacuumed out of a device as it undergoes some inter-pulse maintenance.

Ignoring evacuation for now, the dwell phase involves resetting the central solenoid when the plasma's current is negligible. This corresponds to the secondary of the transformer being an open circuit – fundamentally the central solenoid is the only component. In equation form,

$$V_{max} = \frac{L_1}{\tau_{DW}} \cdot (I_{max} + \tilde{I}) \quad (4.18)$$

Or substituting in \tilde{I} and solving for τ_{DW} ,

$$\tau_{DW} = \frac{L_1}{M} \cdot \frac{(I_{max} \cdot 2M - I_{ID} \cdot L_2)}{V_{max}} \quad (4.19)$$

4.1.3 Specifying Circuit Variables

The goal now is to collect the results from the four phases and introduce the inductance, resistance, voltage, and current terms relevant to our model. This will motivate recasting the problem as flux balance in a reactor – the form commonly used in the literature (and discussed next section).⁷

First, collecting the phase durations in one place:

$$\tau_{RU} = \frac{I_{ID}}{V_{max}} \cdot \left(\frac{L_1 L_2 - M^2}{M} \right) \quad (4.12)$$

$$\tau_{FT} = \frac{I_{max} \cdot 2M - I_{ID} \cdot L_2}{I_{ID} R_P} \quad (4.16)$$

$$\tau_{RD} = \tau_{RU} \quad (4.17)$$

$$\tau_{DW} = \frac{L_1}{M} \cdot \frac{(I_{max} \cdot 2M - I_{ID} \cdot L_2)}{V_{max}} \quad (4.19)$$

These can be used in the definition of the duty-factor: the fraction of time a reactor is putting electricity on the grid. Formulaically,

$$f_{duty} = \frac{\tau_{FT}}{\tau_{pulse}} \quad (4.20)$$

$$\tau_{pulse} = \tau_{RU} + \tau_{FT} + \tau_{RD} + \tau_{DW} \quad (4.21)$$

As will turn out, the solving of pulsed current actually only involves Eq. (4.16). What is interesting about this, is that there is no explicit dependence on ramp-down or dwell! Whereas ramp-up passes \tilde{I} to the flattop phase, the other two are just involved in calculating the duty factor.

The remainder of this subsection will then be defining the following circuit variables: I_{ID} , I_{max} , V_{max} , L_1 , L_2 , and M . Again, the resistance was defined last chapter as:

$$R_P = \frac{K_{RP}}{R_0 \bar{T}^{3/2}} \quad (3.8)$$

The Inductive Current – I_{ID}

The inductive current is what separates pulsed from steady-state operation. It comes from rewriting the current balance given by Eq. (3.3) as:

$$I_{ID} = I_P - (I_{BS} + I_{CD}) \quad (4.22)$$

From before, I_P is the total plasma current in mega-amps, I_{BS} is the bootstrap current, and I_{CD} is the current from LHCD (i.e. lower hybrid current drive). For this model, the relation can be rewritten as:

$$I_{ID} = I_P \cdot \left(1 - K_{CD}(\sigma v)\right) - K_{BS} \bar{T} \quad (4.23)$$

The Central Solenoid Maximums – V_{max} and I_{max}

For this simple model, the central solenoid has two maximum values: the voltage and current. The voltage is the easier to give value. Literature values have this around:⁶

$$V_{max} \approx 5 \text{ kV} \quad (4.24)$$

The maximum current, on the other hand, can be defined through Ampere's Law on a coiled central solenoid:¹¹

$$I_{max} = \frac{B_{CS} h_{CS}}{N \mu_0} \quad (4.25)$$

Here, B_{CS} is a magnetic field strength the central solenoid is assumed to operate at (i.e. 12 T), h_{CS} is the height of the solenoid, N is the number of coils, and μ_0 has its usual physics meaning (i.e. $40 \pi \frac{\mu\text{H}}{\text{m}}$). As will be seen, the value of N does not directly affect the model, as it cancels out in the final flux balance. The height of the central solenoid will, then, be the focus of an upcoming section on improving tokamak geometry.

The Central Solenoid Inductance – L_1

For a central solenoid with circular cross-sections of finite thickness (d), the inductance can be written as:¹²

$$L_1 = G_{LT} \cdot \left(\frac{\mu_0 \pi N^2}{h_{CS}} \right) \quad (4.26)$$

$$G_{LT} = \frac{R_{CS}^2 + R_{CS} \cdot (R_{CS} + d) + (R_{CS} + d)^2}{3} \quad (4.27)$$

Note that R_{CS} is the inner radius of the central solenoid and $(R_{CS} + d)$ is the outer one. In the limit where d is negligible, this says that the inductance is quadratically dependent on the radius of the central solenoid:

$$\lim_{d \rightarrow 0} G_{LT} = G_{LT}^\dagger = R_{CS}^2 \quad (4.28)$$

The formulas for both R_{CS} and d will be defined in a few sections.

The Plasma Inductance – L_2

The plasma inductance is a composite of several different terms, but overall scales with radius. Through equation,

$$L_2 = K_{LP} R_0 \quad (4.29)$$

This static coefficient – K_{LP} – then combines three inductive behaviors of the plasma. The first is its own self inductance (through l_i).⁵ The next is a resistive component through the Ejima coefficient (C_{ejima}), which is usually set to $\sim 1/3$.⁷ And lastly, a geometric component – involving ε and κ – is given by the Hirshman-Neilson model.³³ Mathematically,

$$K_{LP} = \mu_0 \cdot \left(\frac{l_i}{2} + C_{ejima} + \frac{(b_{HN} - a_{HN})(1 - \varepsilon)}{(1 - \varepsilon) + \kappa d_{HN}} \right) \quad (4.30)$$

Here the HN values come from the 1985 Hirshman-Neilson paper:

$$a_{HN}(\varepsilon) = 2.0 + 9.25\sqrt{\varepsilon} - 1.21 \varepsilon \quad (4.31)$$

$$b_{HN}(\varepsilon) = \ln(8/\varepsilon) \cdot (1 + 1.81\sqrt{\varepsilon} + 2.05 \varepsilon) \quad (4.32)$$

$$d_{HN}(\varepsilon) = 0.73\sqrt{\varepsilon} \cdot (1 + 2\varepsilon^4 - 6\varepsilon^5 + 3.7\varepsilon^6) \quad (4.33)$$

The Mutual Inductance – M

The mutual inductance – M – represents the coupling between the solenoid primary and the plasma secondary. A common method for treating this mutual inductance is through a coupling coefficient, k , that links the two self-inductances. Formulaically,

$$M = k\sqrt{L_1 L_2} \quad (4.34)$$

The value of the coupling coefficient, k , is always less than (or equal to) 1, but usually has a value around a third. With all the equations defined, we are now at a position to explain one of the larger nuances of this fusion systems framework: determining the pulse length of a tokamak.

4.1.4 Constructing the Pulse Length

This subsection focuses on a quantitative estimate for how to select a pulse length. As no fusion reactor exists in the world today, the writers believe this is an acceptable calculation. Further, the resulting length of two hours matches the durations of other studies in the literature.^{7,34}

Starting at the end, our goal is to find the pulse length of a tokamak reactor in seconds – as dictated by cyclical stress concerns. The first piece of information is the expected lifetime of the central solenoid, $N \approx 10$ years. The next is the desired

number of pulses the central solenoid will have to last: $M \approx 50,000$ pulses.* This gives a rough estimate of around 10 pulses a day – or a flattop lasting two hours.

With the pulse length defined, we are now in a position to justify neglecting the duty factor for pulsed reactors in this model. Using expected reactor values – while assuming a central solenoid with around 4000 turns – leads to the following scalings:

$$\tau_{FT} \sim \tau_{pulse} \sim \text{O(hours)} \quad (4.35)$$

$$\tau_{RU} \sim \tau_{RD} \sim \tau_{DW} \sim \text{O(mins)} \quad (4.36)$$

As such, even pulsed tokamak reactors should have a duty factor of around unity:

$$f_{duty} \approx 1 \quad (4.37)$$

This analysis of course would change if the central solenoid became an inexpensive component to replace. For example, if a tokamak had a new one installed annually, the pulse length could shorten to be on the order of minutes.

Now that all the terms in a pulsed circuit have been explored, we will move on to rearranging the flattop equation to reproduce flux balance. This will then naturally lead to a generalized current equation – which is the main result of the chapter.

4.2 Producing Flux Balance

The goal of this section is to arrive at a conservation equation for flux balance that mirrors the ones in the literature. The fusion systems model this one attempts to follow most is the PROCESS code.⁷ In a manner similar to power balance, flux balance can be written as:

$$\sum_{sources} \Phi = \sum_{sinks} \Phi \quad (4.38)$$

*This 50,000 pulses is based on the values from the ITER design specifications.³⁴

4.2.1 Rearranging the Circuit Equation

The way to arrive at flux balance from our circuit equations is to rearrange the flattop phase's duration equation:

$$\tau_{FT} = \frac{I_{max} \cdot 2M - I_{ID} \cdot L_2}{I_{ID} R_P} \quad (4.16)$$

Multiplying through by the right-hand side's denominator and moving the negative term over to the left yields:

$$2MI_{max} = I_{ID} \cdot (L_2 + R_P \tau_{FT}) \quad (4.39)$$

This equation is flux balance, where the left-hand side are the sources (e.g. the central solenoid), and the other terms are the sinks (i.e. ramp-up and flattop). The source term can currently be encapsulated within the central solenoid flux:

$$\Phi_{CS} = 2MI_{max} \quad (4.40)$$

The sinks, namely the ramp-up inductive losses (Φ_{RU}) and the flattop resistive losses (Φ_{FT}), are what drain the flux. Here, again, ramp-down and dwell are not included as sinks because flux balance only tracks until the end of flattop. They come into play when measuring the cost of electricity – through the duty factor from Eq. (4.20).

Relabeling terms, flux balance can now be rewritten as:

$$\Phi_{CS} = \Phi_{RU} + \Phi_{FT} \quad (4.41)$$

With the ramp-up and flattop flux given, respectively, by:

$$\Phi_{RU} = L_2 \cdot I_{ID} \quad (4.42)$$

$$\Phi_{FT} = (R_P \tau_{FT}) \cdot I_{ID} \quad (4.43)$$

On comparing these quantities to the ones from the PROCESS paper,⁷ Φ_{RU} and Φ_{FT} are exactly the same. The source terms, on the other hand, are off for two reasons – both related to the central solenoid being the only source term in flux balance. This can partially be remedied by adding the second most dominant source of flux a posteriori – i.e. the PF coils. The second, and inherently limiting factor, is the simplicity of the current model. All that can be shown to this regard is that the Φ_{CS} terms does reasonably predict the values from the PROCESS code.⁸

4.2.2 Adding Poloidal Field Coils

Adding the effect of PF coils – belts of current driving plates on the outer edges of the tokamak – leads to as much as a 50% improvement^{7,8} over relying solely on the central solenoid for flux generation. From the literature, this can be modeled as:¹²

$$\Phi_{PF} = \pi B_V \cdot (R_0^2 - (R_{CS} + d)^2) \quad (4.44)$$

Where again R_{CS} and d are the inner radius and thickness of the central solenoid, respectively. These will be the topic of the next section.

Moving forward, the vertical field – B_V – is a magnetic field oriented up-and-down with the ground. It is needed to prevent a tokamak plasma from drifting radially out of the machine. From the literature, the magnitude of this vertical field (valid for a circular plasma) is given by:⁷

$$|B_V| = \frac{\mu_0 I_P}{4\pi R_0} \cdot \left(\ln \left(\frac{8}{\varepsilon} \right) + \beta_p + \frac{l_i}{2} - \frac{3}{2} \right) \quad (4.45)$$

Analogous to the previously covered plasma beta, the poloidal beta can be represented

by:³⁵

$$\beta_p = \frac{\bar{p}}{\left(\frac{\bar{B}_p}{2\mu_0}\right)} \quad (4.46)$$

Where the average poloidal magnetic field comes from a simple application of Ampere's law:

$$\bar{B}_p = \frac{\mu_0 I_P}{l_p} \quad (4.47)$$

The variable l_p is then the perimeter of the tokamak's cross-sectional halves:

$$l_p = 2\pi a \cdot \sqrt{g_p} \quad (4.48)$$

Here, g_p is another geometric scaling factor,

$$g_p = \frac{1 + \kappa^2(1 + 2\delta^2 - 1.2\delta^3)}{2} \quad (4.49)$$

After a few lines of algebra, this relation for the magnitude of the vertical magnetic field can be written in standardized units as:

$$|B_V| = \left(\frac{1}{10 \cdot R_0}\right) \cdot (K_{VI} I_P + K_{VT} \bar{T}) \quad (4.50)$$

$$K_{VT} = K_n \cdot (\varepsilon^2 g_P) \cdot (1 + f_D) \frac{(1 + \nu_n)(1 + \nu_T)}{1 + \nu_n + \nu_T} \quad (4.51)$$

$$K_{VI} = \ln\left(\frac{8}{\varepsilon}\right) + \frac{l_i}{2} - \frac{3}{2} \quad (4.52)$$

For clarity, this will be plugged into the new PF coil flux contribution (Φ_{PF}):

$$\Phi_{PF} = \pi B_V \cdot (R_0^2 - (R_{CS} + d)^2) \quad (4.44)$$

Which then gets plugged into a more complete flux balance equation:

$$\Phi_{CS} + \Phi_{PF} = \Phi_{RU} + \Phi_{FT} \quad (4.53)$$

The R_{CS} and d terms found in Φ_{PF} will now be discussed as they are needed for this more sophisticated tokamak geometry.

4.3 Improving Tokamak Geometry

From before, this fusion systems model has been said to depend on the major and minor radius: R_0 and a , respectively. Along the way, various geometric parameters have been defined (e.g. ε , κ , δ) to describe the geometry further. Now three more thicknesses will be added – b , c , and d – as well as two fundamental dimension related to the solenoid: its inner radius (R_{CS}) and height (h_{CS}). These are the topics of this section.

4.3.1 Defining Central Solenoid Dimensions

The best way to conceptualize tokamak geometry is through cartoon – see Fig. E-2. What this shows is that there is a gap at the very center of a tokamak. This gap extends radially outwards to R_{CS} meters where the coiled central solenoid – of thickness d – begins. Between the outer edge of the solenoid and the wall of the torus (i.e. the doughnut) are the blanket and toroidal field (TF) coils.

The blanket and TF coils have thicknesses of b and c , respectively. Before defining b , c , and d , however, it proves useful to relate them all inside equations for the inner radius (R_{CS}) and height (h_{CS}) of the central solenoid.

$$R_{CS} = R_0 - (a + b + c + d) \tag{4.54}$$

$$h_{CS} = 2 \cdot (\kappa a + b + c) \tag{4.55}$$

Again, this relation is pictorially represented in Fig. E-2. The next step is defining: b , c , and d – to close the variable loop.

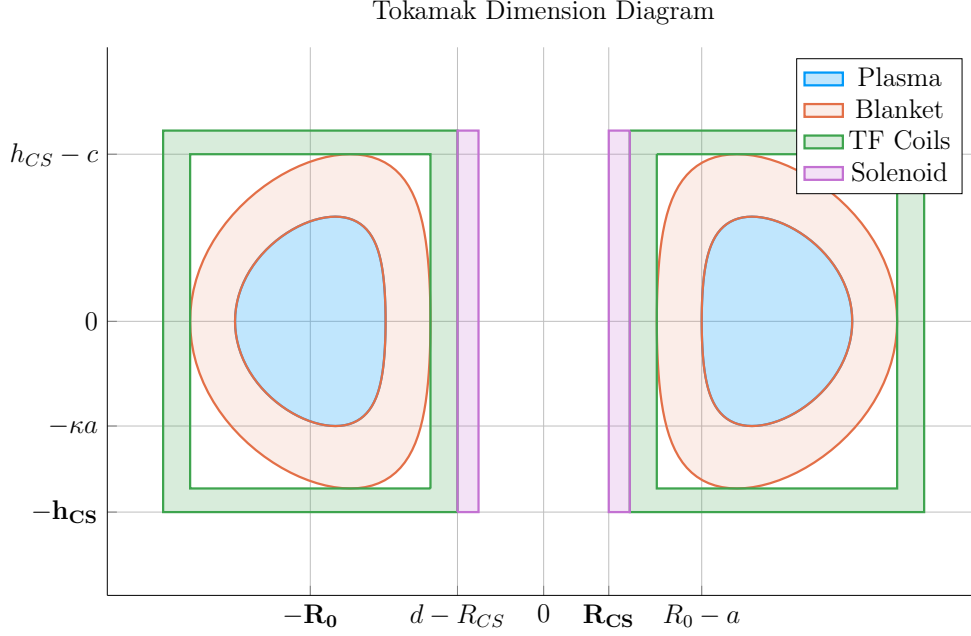


Figure 4-3: Dimensions of Tokamak Cross-Section

Geometrically, a tokamak consists mainly of four components: the plasma, its metallic blanket, the toroidal field magnets surrounding them, and the central solenoid. These have thicknesses of a , b , c and d , respectively. R_{CS} is where the solenoid begins.

4.3.2 Calculating Component Thicknesses

In between the inner surface of the central solenoid and the major radius of the tokamak are four thicknesses: a , b , c , and d . This subsection will go over them one at a time.

The Minor Radius – a

The minor radius was the first of these thicknesses we encountered. To calculate it, we introduced the inverse aspect ratio (ε) to relate it to the major radius (R_0):

$$a = \varepsilon \cdot R_0 \quad (2.1)$$

The Blanket Thickness – b

The blanket is an area between the TF coils and the torus that is composed mainly of lithium and steel. It serves to both: protect the superconducting magnet structures from neutron damage, as well as breed more tritium fuel from stray fusion neutrons.³⁶ In equation form, the blanket thickness is given by:¹³

$$b = 1.23 + 0.074 \ln P_W \quad (4.56)$$

Here, P_W is a small correction to account for extra wall loading (as discussed in Section 3.4.3). Most blankets are usually around a meter.^{6,13}

Moving forward, the remaining two thicknesses – c and d – are handled differently: estimating structural steel portions as well as magnetic current-carrying ones.

The Toroidal Field Coil Thickness – c

The thickness of the TF coils – c – is a little beyond the scope of this paper. It does, however, have a form that combines a structural steel component with a magnetic portion. From a previous model, this can be given as:¹³

$$c = G_{CI}R_0 + G_{CO} \quad (4.57)$$

$$G_{CI} = \frac{B_0^2}{4\mu_0\sigma_{TF}} \cdot \frac{1}{(1 - \varepsilon_b)} \cdot \left(\frac{4\varepsilon_b}{1 + \varepsilon_b} + \ln \left(\frac{1 + \varepsilon_b}{1 - \varepsilon_b} \right) \right) \quad (4.58)$$

$$G_{CO} = \frac{B_0}{\mu_0 J_{TF}} \cdot \frac{1}{(1 - \varepsilon_b)} \quad (4.59)$$

The critical stress – σ_{TF} – in G_{CI} implies it depends on the structural component, whereas the maximum current density – J_{TF} – implies a magnetic predisposition in G_{CO} . The use of G_{\square} in these quantities, instead of K_{\square} is because they include

the toroidal magnetic field strength: B_0 . For this reason, they are referred to as dynamic coefficients. Lastly, the term ε_b represents the blanket inverse aspect ratio that combines the minor radius with the blanket thickness:

$$\varepsilon_b = \frac{a + b}{R_0} \quad (4.60)$$

The Central Solenoid Thickness – d

Finishing this discussion where we started, the central solenoid's thickness – d – has a form similar to the TF coils (i.e. c). It can be represented as:¹³

$$d = K_{DR}R_{CS} + K_{DO} \quad (4.61)$$

$$K_{DR} = \frac{3B_{CS}^2}{6\mu_0\sigma_{CS} - B_{CS}^2} \quad (4.62)$$

$$K_{DO} = \frac{6B_{CS}\sigma_{CS}}{6\mu_0\sigma_{CS} - B_{CS}^2} \cdot \left(\frac{1}{J_{OH}} \right) \quad (4.63)$$

Here, the use of K_{\square} for the coefficients signifies their use as static coefficients. Therefore, B_{CS} must be treated as a static variable representing the magnetic field strength in the central solenoid. For prospective solenoids using high temperature superconducting (HTS) tape, B_{CS} may be around 20 T. The values of σ_{CS} and J_{CS} have similar meanings to the ones for TF coils. These are collected in Table 4.2 with example values representative of our model.

Before moving on, it seems important to say that although K_{DI} and K_{DO} do not

Table 4.2: Example TF Coils and Central Solenoid Critical Values

(a) Stresses [MPa]			(b) Current Densities [MA/m ²]		
Item	Symbol	Limit	Item	Symbol	Limit
Solenoid	σ_{CS}	600	Solenoid	J_{CS}	100
TF Coils	σ_{TF}	600	TF Coils	J_{TF}	200

depend on dynamic variables, R_{CS} most definitely does. This is what makes the central solenoid's thickness difficult.

4.3.3 Revisiting Central Solenoid Dimensions

Now that the various thicknesses have been defined (i.e. a , b , c , and d), the equations for the solenoid's dimensions – R_{CS} and h_{CS} – can be revisited and simplified. From before,

$$R_{CS} = R_0 - (a + b + c + d) \quad (4.54)$$

$$h_{CS} = 2 \cdot (\kappa a + b + c) \quad (4.55)$$

Repeated, the four thicknesses in these equations are:

$$a = \varepsilon \cdot R_0 \quad (2.1)$$

$$b = 1.23 + 0.074 \ln P_W \quad (4.56)$$

$$c = G_{CI}R_0 + G_{CO} \quad (4.57)$$

$$d = K_{DR}R_{CS} + K_{DO} \quad (4.61)$$

Substituting these thicknesses into the central solenoid's dimensions results in:

$$h_{CS} = 2 \cdot (R_0 \cdot (\varepsilon \kappa + G_{CI}) + (b + G_{CO})) \quad (4.64)$$

$$R_{CS} = \frac{1}{1 + K_{DR}} \cdot (R_0 \cdot (1 - \varepsilon - G_{CI}) - (K_{DO} + b + G_{CO})) \quad (4.65)$$

These are the complete central solenoid dimension formulas. To make them more

tractable to the reader, they will now be simplified one step at a time.*

The first simplification to make while estimating central solenoid dimensions is to neglect the magnetic current-carrying portions of the central solenoid and TF coils. This results in:

$$\lim_{\substack{G_{CO} \rightarrow 0 \\ K_{DO} \rightarrow 0}} h_{CS} = h_{CS}^{\dagger} = 2R_0 \cdot (K_{EK} + \varepsilon_b + G_{CI}) \quad (4.66)$$

$$\lim_{\substack{G_{CO} \rightarrow 0 \\ K_{DO} \rightarrow 0}} R_{CS} = R_{CS}^{\dagger} = \frac{R_0}{1 + K_{DR}} \cdot (1 - \varepsilon_b - G_{CI}) \quad (4.67)$$

The new static coefficient, here, is:

$$K_{EK} = \varepsilon \cdot (\kappa - 1) \quad (4.68)$$

The next simplification is ignoring the TF coil thickness – and thus magnetic field dependence – altogether:

$$\lim_{G_{CI} \rightarrow 0} h_{CS}^{\dagger} = h_{CS}^{\ddagger} = 2R_0 \cdot (K_{EK} + \varepsilon_b) \quad (4.69)$$

$$\lim_{G_{CI} \rightarrow 0} R_{CS}^{\dagger} = R_{CS}^{\ddagger} = \frac{R_0}{1 + K_{DR}} \cdot (1 - \varepsilon_b) \quad (4.70)$$

These oversimplifications will be used later this chapter while simplifying the generalized current equation to something more tractable. For now, they highlight how the dimensions change as different components are neglected. The next step is bringing plasma physics back into flux balance and solving for the generalized current.

*The same simplification exercise will be done again after the generalized current is derived later this chapter.

4.4 Piecing Together the Generalized Current

The goal of this section is to quickly expand flux balance using all the defined quantities and then rearrange it into an equation for plasma current – which is suitable for root solving. This starts with a restatement of flux balance in a reactor:

$$\Phi_{CS} + \Phi_{PF} = \Phi_{RU} + \Phi_{FT} \quad (4.53)$$

$$\Phi_{CS} = 2MI_{max} \quad (4.40)$$

$$\Phi_{PF} = \pi B_V \cdot (R_0^2 - (R_{CS} + d)^2) \quad (4.44)$$

$$\Phi_{RU} = L_2 \cdot I_{ID} \quad (4.42)$$

$$\Phi_{FT} = (R_P \tau_{FT}) \cdot I_{ID} \quad (4.43)$$

The first step is realizing that the central solenoid flux can now be rewritten using the new geometry in a standardized form:

$$\Phi_{CS} = K_{CS} \cdot \sqrt{R_0 G_{LT} h_{CS}} \quad (4.71)$$

$$K_{CS} = 2k B_{CS} \cdot \sqrt{\frac{\pi K_{LP}}{\mu_0}} \quad (4.72)$$

Next, we will slightly simplify the PF coil flux using a dynamic variable coefficient:

$$\Phi_{PF} = G_V \cdot \frac{K_{VI} I_P + K_{VT} \bar{T}}{R_0} \quad (4.73)$$

$$G_V = \frac{\pi}{10} \cdot (R_0^2 - (R_{CS} + d)^2) \quad (4.74)$$

This allows us to rewrite the generalized current as:

$$I_P = \frac{(K_{BS} + G_{IV}/G_{IP}) \cdot \bar{T}}{1 - K_{CD}(\sigma v) - G_{ID}/G_{IP}} \quad (4.75)$$

$$G_{IU} = K_{VT} G_V + K_{CS} R_0^{3/2} \cdot \frac{\sqrt{h_{CS} G_{LT}}}{\bar{T}} \quad (4.76)$$

$$G_{ID} = K_{VI} G_V \quad (4.77)$$

$$G_{IP} = K_{LP} R_0^2 + \frac{K_{RP} \tau_{FT}}{\bar{T}^{3/2}} \quad (4.78)$$

As we will show in the next section, this form not only has a form remarkably similar to the steady current – it reduces to it in the limit of infinitely long pulses!

4.5 Simplifying the Generalized Current

This section focuses on making various simplifications to the generalized current:

$$I_P = \frac{(K_{BS} + G_{IU}/G_{IP}) \cdot \bar{T}}{1 - K_{CD}(\sigma v) - G_{ID}/G_{IP}} \quad (4.75)$$

As promised, this will start with the trivial simplification of the generalized current into steady state. Next it will move on to a basic simplification for the purely pulsed case. These two activities should shed some light on how to interpret the equation in the more complicated hybrid case (actually used by the model).

4.5.1 Recovering the Steady Current

The place to start with the steady current simplification is in the dynamic coefficient, G_{IP} :

$$G_{IP} = K_{LP} R_0^2 + \frac{K_{RP} \tau_{FT}}{\bar{T}^{3/2}} \quad (4.78)$$

As can be seen, as $\tau_{FT} \rightarrow \infty$, so does the coefficient,

$$\lim_{\tau_{FT} \rightarrow \infty} G_{IP} = \infty \quad (4.79)$$

Because G_{IU} and G_{ID} remain constant, their contribution to plasma current becomes insignificant in this limit. Concretely,

$$\lim_{\tau_{FT} \rightarrow \infty} I_P = \frac{K_{BS} \bar{T}}{1 - K_{CD}(\sigma v)} \quad (4.80)$$

This is precisely the steady current given by Eq. (2.28)! The generalized current automatically works when modeling steady-state tokamaks.*

4.5.2 Extracting the Pulsed Current

For pulsed reactors, we have to resolve a similar problem – except now τ_{FT} is expected to be a reasonably sized number (i.e. 2 hours).

With an aim at intuition, the reactor is first treated as purely pulsed – having no current drive assistance:

$$\lim_{\eta_{CD} \rightarrow 0} I_P = \frac{(K_{BS} + G_{IU}/G_{IP}) \cdot \bar{T}}{1 - (G_{ID}/G_{IP})} \quad (4.81)$$

Next, for simplicity-sake, the PF coil contribution to flux balance is assumed negligible, as it was always meant to be a correction term:

$$\lim_{\Phi_{PF} \ll \Phi_{CS}} G_{IU} = K_{CS} R_0^{3/2} \cdot \frac{\sqrt{h_{CS} G_{LT}}}{\bar{T}} \quad (4.82)$$

$$\lim_{\Phi_{PF} \ll \Phi_{CS}} G_{ID} = 0 \quad (4.83)$$

Piecing this altogether, we can write a new current for this highly simplified case,

$$I_P^\dagger = K_{BS} \bar{T} + \frac{K_{CS} R_0^{3/2} \cdot \sqrt{h_{CS} G_{LT}}}{K_{LP} R_0^2 + K_{RP} \tau_{FT} \bar{T}^{-3/2}} \quad (4.84)$$

*It should be noted that this is much harder when setting τ_{FT} to a large, but finite number – as η_{CD} still needs to be solved self-consistently.

As this is not quite simple enough, these previous simplifications will be incorporated:

$$G_{LT}^{\dagger} = R_{CS}^2 \quad (4.28)$$

$$h_{CS}^{\dagger} = 2R_0 \cdot (K_{EK} + \varepsilon_b) \quad (4.69)$$

$$R_{CS}^{\dagger} = \frac{R_0}{1 + K_{DR}} \cdot (1 - \varepsilon_b) \quad (4.70)$$

Taking these into consideration results in the following current formula:

$$I_P^{\dagger} = K_{BS} \bar{T} + \left(\frac{K_{CS} R_0^3}{K_{LP} R_0^2 + K_{RP} \tau_{FT} \bar{T}^{-3/2}} \cdot \frac{(1 - \varepsilon_b) \cdot \sqrt{2(K_{EK} + \varepsilon_b)}}{1 + K_{DR}} \right) \quad (4.85)$$

In the limit that the pulse length drops to zero (and bootstrap current is negligible),

$$\lim_{\tau_{FT} \rightarrow 0} I_P^{\dagger} = R_0 \cdot \left(\frac{K_{CS}}{K_{LP}} \cdot \frac{(1 - \varepsilon_b) \cdot \sqrt{2(K_{EK} + \varepsilon_b)}}{1 + K_{DR}} \right) \quad (4.86)$$

This implies that a purely pulsed current scales with major radius to leading order.

4.5.3 Rationalizing the Generalized Current

From the previous two subsections, we arrived at equations for infinitely large and infinitely small pulse lengths:

$$\lim_{\tau_{FT} \rightarrow \infty} I_P = \frac{K_{BS} \bar{T}}{1 - K_{CD}(\sigma v)} \quad (4.80)$$

$$\lim_{\tau_{FT} \rightarrow 0} I_P^{\dagger} = R_0 \cdot \left(\frac{K_{CS}}{K_{LP}} \cdot \frac{(1 - \varepsilon_b) \cdot \sqrt{2(K_{EK} + \varepsilon_b)}}{1 + K_{DR}} \right) \quad (4.86)$$

What these imply at an intuitive level is that at small pulses, current scales with the major radius. While for long pulses, current scales with plasma temperature. In the general case, of course, the problem becomes much harder to predict – as shown by the code’s results using Eq. (4.75).